# 3. Methodology

## 3.1 General

This chapter deals with the standard methodology for undertaking different components of the study. Figure 3.1 depicts the generalised methodology for the development of an approach for the design of PWBP to acceptable engineering standards. It consisted of an extensive field survey followed by a literature review and laboratory tests that formed the essential preparatory work for this study.

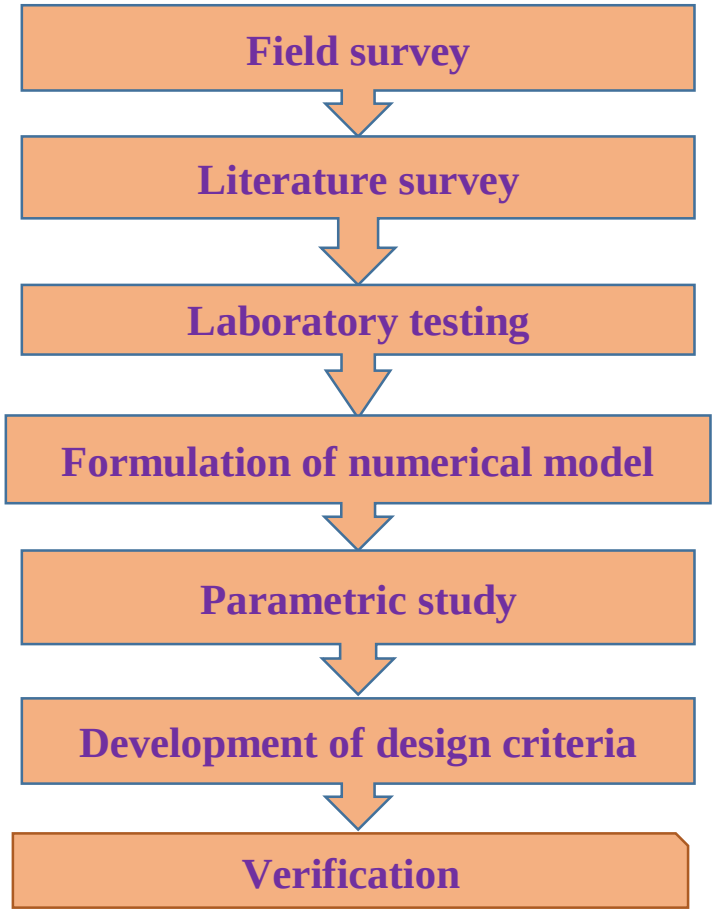


**Figure 3.1.** Research methodology

In the second stage, a hydro-mechanically coupled model was worked out to assess the performance of PWBP. It considered the laboratory-calibrated strain-softening properties of the coal simulating the load-deformation behaviour of the coal pillars having different w/h ratios, the effect of water on residual cohesion and friction, mobilization of dilation with plastic shear strain and updating induced permeability and flow vector based on the induced volumetric strain and pore pressure as a function of the redistributed stress and failure condition of the rock mass forming the pillar.

## 3.2 Preparatory Work

The preparatory work included an extensive field survey, literature review and laboratory test. The field survey of the existing PWBP mine sites was conducted to study the hydro-mechanical performance of PWBPs in different geo-mining conditions. The data were compiled in terms of the cover depth, PWBP width, water head, and seepage rate in Table 1.1, Chapter 1. This data formed the basis for the parametric study, as discussed in Chapter 4.

The field survey was followed by an in-depth literature review to study the existing design approaches and the associated aspects of pillar design. The outcome of this study, as compiled in Chapter 2, helped in orienting the research efforts to address the prevailing knowledge gap. The laboratory testing evaluated the peak compressive strength and the post-failure behaviour of coal samples with a w/h ratio varying from 0.5–10 to assess their load–deformation behaviour. All these tests were done in a stiff testing system at the Rock Mechanics Laboratory of the Department of Mining Engineering, IIT (BHU) Varanasi. The details are mentioned in Section 4.1, Chapter 4.

## 3.3 Numerical Modelling

The literature review revealed that numerical modelling could offer valuable insight into the design of barrier pillars. It is also the most efficient way of researching a ground control problem. When implemented with one or more other methods, it yields substantial insight into a given circumstance. It considers regional and localised pillar systems (roof-pillar-floor) accurately along with the pre-mining stress environment, material properties, mining-induced changes, and loading rate effects to assess the mode and location of the failure and offers faster parametric studies for quantitative assessment of critical parameters. The methodology for numerical modelling for the assessment of the mechanical and hydraulic performance of a PWBP in a given condition is depicted in the form of a flow chart, as shown in Figure 3.2. A detailed description of the flow chart is given in the following sections.

A field representative constitutive behaviour of the pillars for the mechanical loading was ensured before simulating the hydro-mechanical coupled phenomenon. In the first stage, the strain-softening parameters were established to simulate the laboratory-observed lab deformation behaviour of coal specimens having a w/h ratio varying from 0.5-13.5. This study was done with particular reference to Das (1986) for six Indian coal seams in addition to the laboratory test conducted in this study. The post-failure behaviour, such as peak strength, post-failure modulus, and residual strength of the coal material, depends on the strain-softening parameters and the zone size of the discretized elements. Hence, the model parameters were calibrated to establish the best-fit relationships for estimating the drop rate and the residual values of cohesion and friction angle to simulate the laboratory-observed behaviour.

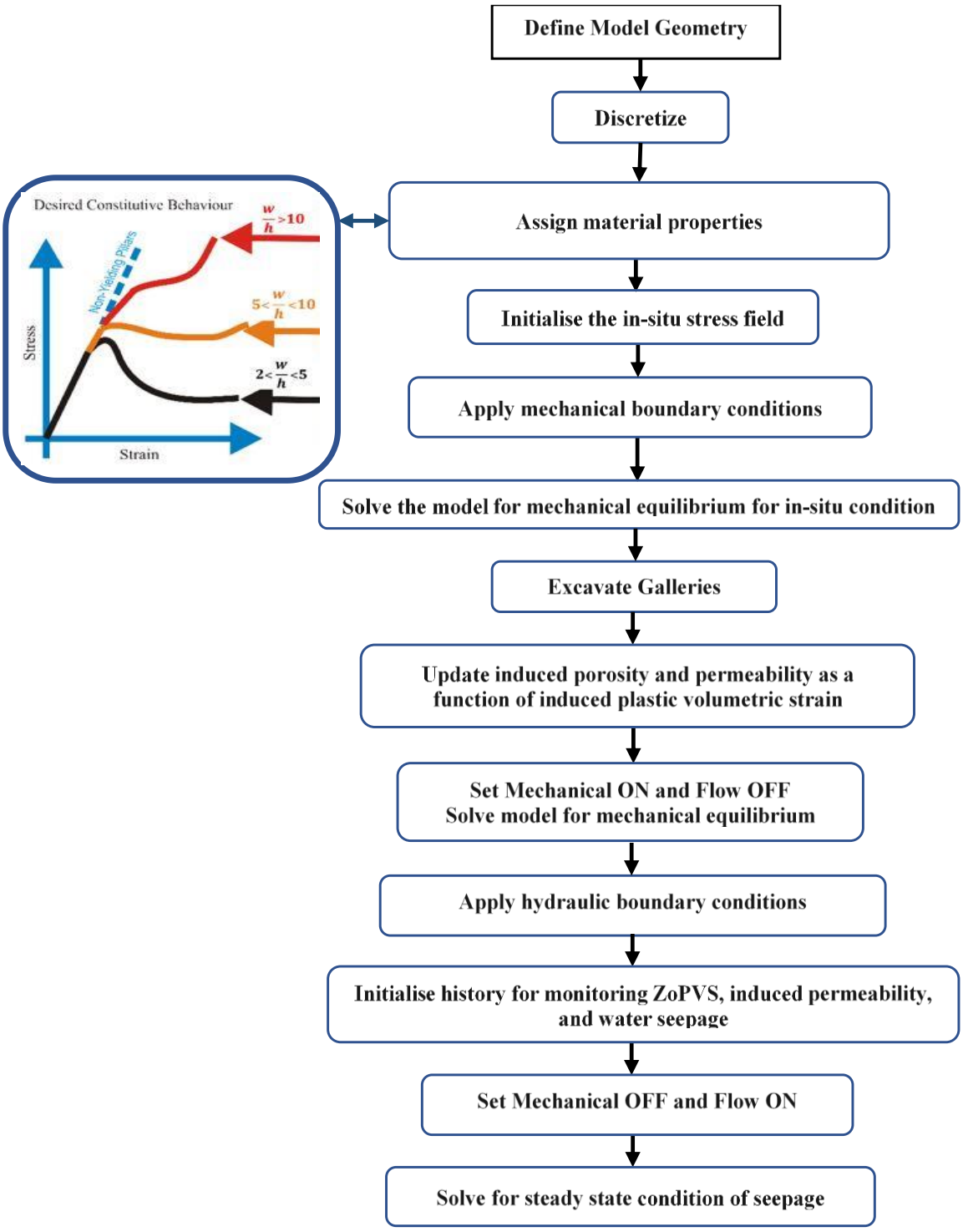


**Figure 3.2.** Methodology of numerical simulation for the mechanical-hydraulic coupled modelling of Protective Water Barrier Pillars

The modelling study was done using the Finite Difference code FLAC 2D (ITASCA, 2011). It was considered that the dynamically moving fluid in a porous media alters the mechanical response of the structure. An increase in pore pressure causes rock dilatation, and the rock compression induces increased pore pressure if the fluid cannot escape the pore network. The mechanical properties of the rock are time-dependent due to these linked processes. Hence, a study state solution was obtained to assess the mechanical damage and the resultant water seepage rate through the barrier in all conditions.

### 3.3.1 Model Formulation

Formulation of the numerical model of the PWBP comprised defining an appropriate model geometry, and its discretization, assigning constitutive behaviour and material properties for rock mass and the interface between the roof-pillar-floor, initialising in-situ stresses and applying boundary conditions. Histories were defined to monitor the changes in desired parameters, such as unbalanced force, major and minor principal stresses, induced volumetric strain, permeability, and water seepage rate across the barrier. It also incorporated FISH sub-routines to control model behaviour using user-defined functions and monitor their outcome.

### 3.3.2 Model Geometry

The model geometry of a pillar system consisted of a 50 m thick roof and floor sandwiching a 3 m thick coal seam and interfaces at material transition planes. Sub-regions equal to twice the mining height were considered in the roof and floor to accommodate the worst possible effect of excavation in the coal seam. These sub-regions, as considered in the roof and floor, were named 'ZoI_Roof' and 'ZoI_Floor', respectively, in this thesis. The effect of remaining strata above the 50 m thick roof was incorporated by applying equivalent in-situ vertical stress over the upper boundary of the model. The width of the model was varied with the

changing width of the PWBP and the gallery. The gallery width was fixed as 5 m in all cases. A schematic diagram for model geometry is shown in Figure 3.3.

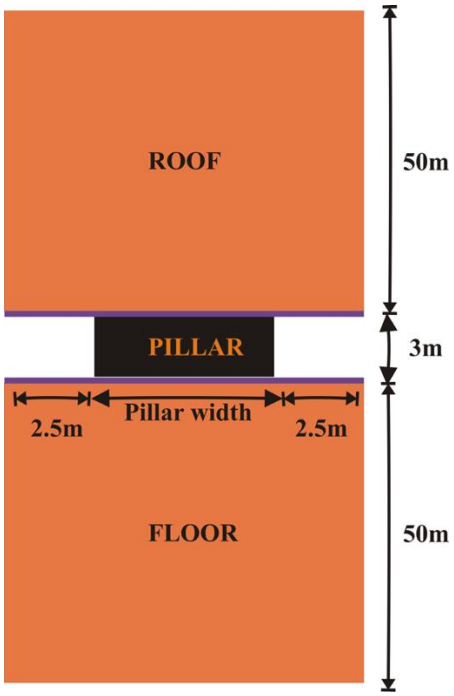


**Figure 3.3.** Schematic diagram of model geometry

The elements forming the 'Pillar', 'ZoI_Roof', and 'ZoI_Floor' were combinedly termed as 'Model_Zone_of_Interest' (MZoI). The width of the pillar and the gallery governed the width of MZoI, whereas the height of the MZoI was dependent on the flow regimes. It was only 3 m for the 'pillar-only' cases, 6 m for 'roof-only' and 'floor-only' cases, 9 m for the 'pillar-roof-only' and the 'pillar-floor only' cases, and 15 m for the 'pillar system' that considered flow through the MZoI. The top and bottom boundaries were selected 50 m away from the excavation so that boundaries remain unaffected due to the disturbances in the MZoI.

The element size in the X and Y directions was kept constant in all the models, as the model outcomes were dependent on the zone size. The X-axis was considered aligned to the horizontal plane, and the Y-axis to the vertical plane in the model. The origin (0,0) was fixed at the bottom left corner of the model. The number of zones in the model was defined for the constant element size of 0.5 m × 0.5 m. This zone size was optimised considering the requirement of small-size grids for the strain-softening constitutive model. Two hundred eight zones were created in the Y direction of the model. The first 100 zones from the origin formed the floor, the next zone accommodated the interface between the coal seam and the floor, followed by the subsequent six zones that formed the coal seam, one zone accommodating the interface between the coal seam and roof, and remaining 100 zones forming the roof. The number of zones varied in the X direction, depending on the pillar width, to ensure the same element size across different models. A schematic diagram of model geometry, along with the model's origin, axis, and grids, is shown in Figure 3.4.

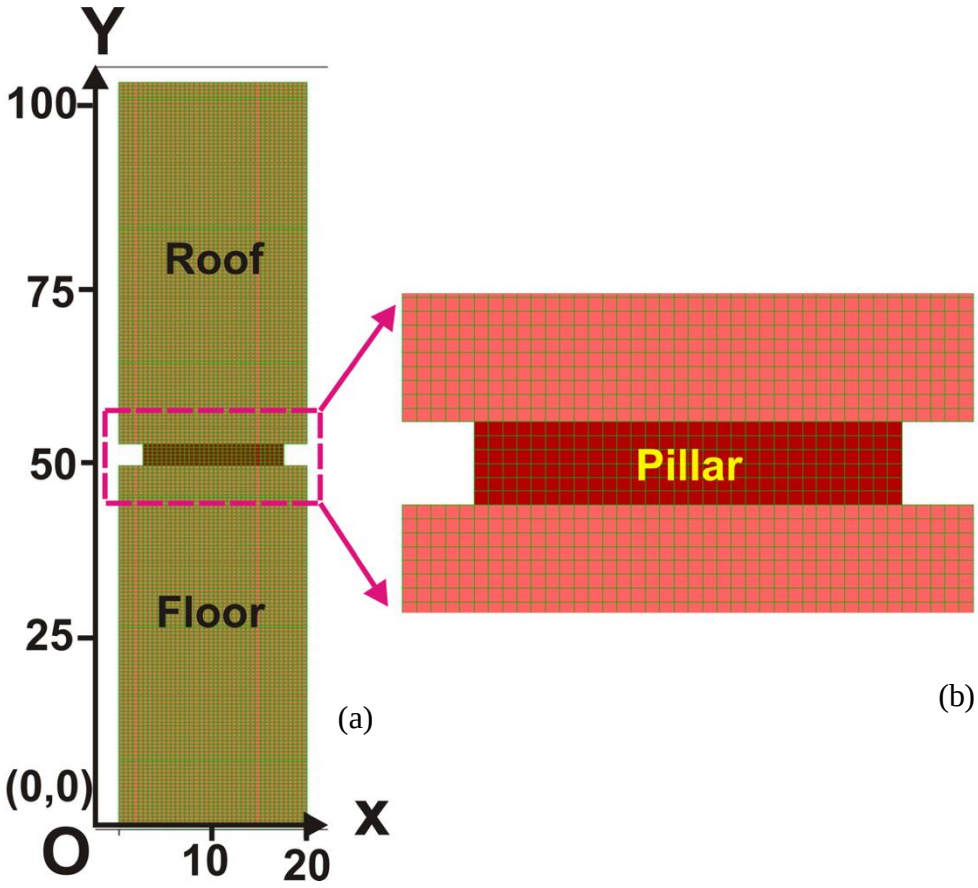


**Figure 3.4.** (a) Model geometry showing origin (0,0), x and y axes, and uniform zone size, (b) magnified part of MzoI

### 3.3.3 Interface Behaviour

Interface is a built-in feature available in FLAC software that can be used to model sliding and separation between two planes (ITASCA, 2011). The findings of Prassetyo et al. (2019), Viktor Lonnies (2017), Rashed and Peng (2015), and ITASCA (2011) were analysed to estimate the interface properties. The FLAC manual (ITASCA, 2011) suggested interface cohesion varying from zero to the uniaxial compressive strength of the surrounding material. Lonnies (2017) observed that most of the coal-rock interfaces have clay infill material, which can easily be washed away by water under high pressure. In consideration of the above, we considered zero cohesion for the coal-rock interface for a realistic simulation of the hydro-

mechanical interaction of the protective water barrier. The tensile strength of the interface was also considered to be zero for a similar reason. The ITASCA (2011) suggested range of interface friction angle varied between 5–25°, and the normal and shear stiffness varied from 10-100 MPa/m. However, it is crucial to assign a reasonable stiffness to control the inter-penetration within the permissible limit of 10 times the minimum zone size on either side of the interface for realistic simulation of soft slip planes. Accordingly, the stiffness estimated by Equation 3.1 (ITASCA, 2011), along with the friction angle of 14° and the dilation angle of 5°, was used to simulate the roof-pillar-floor interfaces in this study. The properties for calculating stiffness should be of the softer material between the two sides of an interface.

$$10max\left[\frac{\left(K+\frac{4}{3}G\right)}{\Delta z_{min}}\right] \quad \ldots(3.1)$$

Where $\Delta z_{min}$ = minimum zone size, m

G = shear modulus, GPa and

K = Bulk modulus, GPa.

### 3.3.4 Constitutive Model

Initially, the elastic constitutive model was assigned to the pillar system and solved for equilibrium for a controlled and smooth transition of the unbalanced force to an equilibrium state. Subsequently, the Mohr-Coulomb model was introduced to simulate the behaviour of the roof and floor strata, while the coal pillar was modelled using the strain-softening model. The peak strength, post-failure modulus, and residual strength of a material depend on strain-softening parameters, including the zone size. The model parameters, calibrated with the

laboratory findings for w/h ratio varying from 0.5 to 13.5 for the Indian coal seams (Equation 4.1-4.4, Chapter 4), were incorporated for realistic modelling of the pillar behaviour. The variation in the dilation angle was incorporated using Equations 2.11-2.15, as suggested by Walton and Diederich (2015). The dilation-dependent control of plastic volumetric strain was implemented in the model through an in-house developed FISH module. The 'null' model was assigned to excavate the galleries and develop the barrier pillar in the models.

The initial results of the initial hydro-mechanically coupled model indicated that the flow regime against a given water head was not representative of the conditions prevailing in the field. Hence, appropriate refinement in the model was needed to simulate the effect of plastic strain on the residual cohesion under the influence of water pressure and their combined impact on the induced porosity and the permeability of the rock matrix. Finally, such an improved model could be developed by implementing 100 % cohesion weakening at 1% plastic strain in the pillar.

For steady-state coupled numerical simulation of porous rocks, the 'CONFIG gwflow' mode was used at the beginning to configure the model grids for fluid flow analysis. At the same time, the model was also configured for automatic adjustment of effective stresses using the 'CONFIG ats' command. The fluid flow solution was based on the grid point pore pressure, and effective stresses were based on the zone pore pressure, calculated as the average of the grid point pore pressure.

The simulation of the porous media can be sluggish with a simplified basic flow scheme when the fluid bulk modulus is larger compared to the drained bulk modulus of the porous medium or when there is a considerable variation in porosity, permeability, or grid size.

Hence, the fast-flow technique was invoked in this study using the command 'SET funsat on' to facilitate faster convergence of the solution.

### 3.3.5 Estimation of Mechanical and Hydraulic Properties

Various researchers have made efforts to accommodate the effect of rock mass heterogeneity and discontinuities for estimating the rock mass properties from the laboratory-measured intact rock properties. RMR and GSI-based approaches are the most common. However, obtaining a fair estimate of these indices under laboratory conditions is challenging and requires considerable validation to remove subjectivity before a large-scale acceptance. Considering these practical difficulties, the approach suggested by Singh and Singh (2009) was used in this work for estimating the rock mass strength properties and modulus of elasticity as it has proven worthy to reflect the field observed behaviour of strata in the Indian geo-mining conditions very closely (Behera, et al., 2021; Sahoo et al., 2020). The rock mass compressive and tensile strengths were estimated by multiplying a scale-down factor of 50% and the RQD to the intact compressive and tensile strengths. The modulus of elasticity for the rock mass was taken the same as the intact rock modulus. The approach suggested by Wilson (1980) was used to estimate the elastic modulus of rock in the absence of laboratory-tested data. The modulus of elasticity (GPa) was calculated as 0.31 times the compressive strength (MPa), except for coal, which was considered constant as 2 GPa. A thickness-weighted average approach was used to estimate strength and deformation modulus properties for rock layers composed of different rock beds.

The friction angle of 25° was reckoned for coal and 40° for other rock masses. The initial dilation angle for coal was considered as zero and 5° for other rock mass and was updated based on plastic volumetric strain in the MZoI as explained above. The Poison's ratio for

coal was 0.25 and 0.35 for other rocks. The shear modulus (G), bulk modulus (B), and cohesion (C) were estimated using standard relations (ITASCA, 2011).

The mobility coefficient and porosity are the critical parameters for the modelling of water seepage rate. The mobility coefficient is defined as the ratio of the permeability of the flow medium to the dynamic viscosity of the fluid. Equation 3.2, as suggested by ITASCA (2011), was used for simulating changes in porosity as a function of the induced volumetric strain in the rock matrix. Similarly, the mobility coefficient was updated as a function of the volumetric strain using Equation 3.3, as suggested by Zhu et al. (2015).

$$n = 1 - \frac{1-n_o}{1+e_v} \quad \ldots(3.2)$$

$$k = k_o \left[\left\{\left(\frac{1}{n_o}\right)(1+e_v)^3\right\} - \left\{\left(\frac{1-n_o}{n_o}\right)(1+e_v)^{-1/3}\right\}\right]^3 \quad \ldots(3.3)$$

Where k = induced mobility coefficient in $m^2$/Pa.sec,

n = induced porosity,

$n_o$ = initial porosity,

$e_v$ = induced volumetric strain, and

$k_o$ = in-situ mobility coefficient in $m^2$/Pa.sec.

The porosity and permeability values were updated as the function of induced volumetric strain. FISH functions were developed to generate tables for implementing the variation of porosity and mobility coefficients as functions of accumulated volumetric strain. The negative volumetric strain in these tables represented the compression, while the positive

value represented the tension. The induced porosity and permeability distribution were updated every ten time-steps as rapid changes affected the critical timestep, and recalculating hydraulic quantities was also time-consuming.

### 3.3.6 Estimation of In-situ Stress Field and its Initialisation

In the absence of field-measured in-situ stress data, the in-situ vertical stress for working was estimated using the gravity loading approach (Equation 3.4), while the mean in-situ horizontal stress was estimated using Sheorey (1994) elasto-static thermal stress model (Equation 3.5) for Indian geo-mining conditions.

$$\sigma_v = \gamma D \quad \ldots(3.4)$$

$$\sigma_h = \frac{\vartheta}{1-\vartheta}\gamma \mathrm{D} + \frac{\beta \mathrm{EG}}{1-\vartheta}(\mathrm{D} + 1000) \quad \ldots(3.5)$$

Where, $\sigma_v$ = vertical stress, MPa,

$\gamma$ = unit weight of rock, MPa/m,

D = cover depth, m,

$\sigma_h$ = mean horizontal stress, MPa,

$\vartheta$ = Poisson's ratio,

$\beta$ = coefficient of thermal expansion of rock ($30 \times 10^{-6}$/ºC for coal, $8 \times 10^{-6}$/ºC for sandstone),

G = average geothermal gradient for Indian coalfields (0.03ºC /m).

### 3.3.7 Boundary Conditions

The mechanical boundary conditions were initialized in the model before solving it for in-situ equilibrium. A roller boundary condition was applied to the vertical boundary at the two sides and a rigid boundary to the floor, as shown in Figure 3.5.

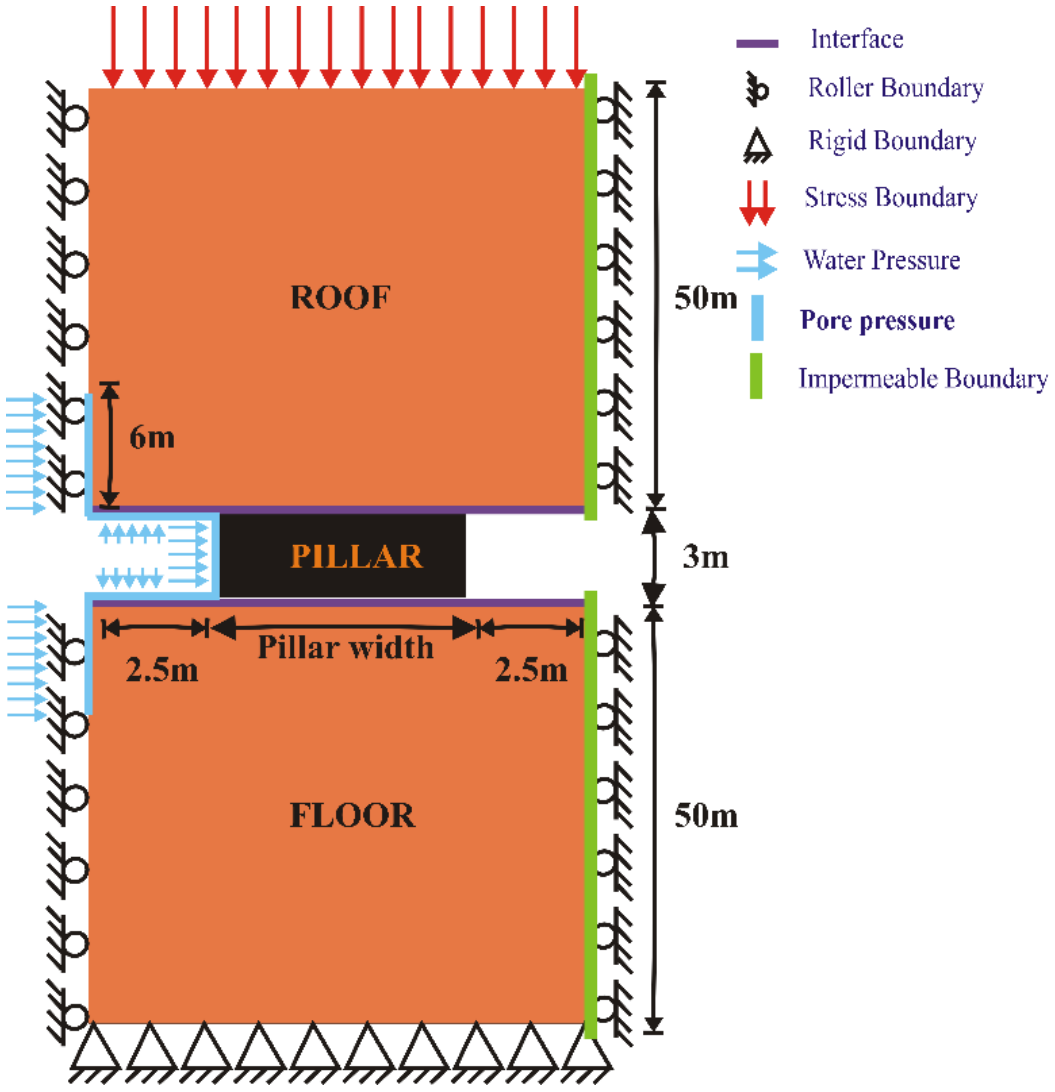


**Figure 3.5.** Model geometry showing mechanical and hydraulic boundary conditions

The hydraulic boundary conditions were prescribed after attaining the mechanical equilibrium upon the development of the pillar. The left-hand side of the pillar formed after excavation demarcated the reservoir, and the other side of the pillar represented the active mine working. The saturated boundary condition and equivalent pore pressure estimated by Equation 3.6 were applied on the reservoir side vertical and horizontal edges formed within the excavated region and up to 6 m below and above the water barrier pillar on the vertical boundary of the model, depending upon the flow regime. The vertical boundaries were considered impermeable beyond the pillar on the active side of the mine working.

$$p = \gamma_w H \qquad \ldots(3.6)$$

Where, p = water pressure, Pa,

$\gamma_w$ = unit weight of water, Pa/m, and

H = water head, m.

### 3.4 Modelling Scheme

The numerical model of PWBP considered only its mechanical loading till the achievement of the equilibrium condition during the development of the pillar. The model was solved to mechanical equilibrium to assess the induced changes in the mechanical and hydraulic parameters and their coupled interactions.

Subsequently, the hydraulic boundary conditions were imposed to solve for seepage rate through the pillar. The equilibrium condition for steady-state analysis was monitored using the FISH function 'QRATIO.FIS' already available in the FISH library of the software. This FISH function computes 'qratio', a dimensionless number, as the difference between the

absolute value of the total inflow and outflow using the FISH grid variable 'gflow', which measures the total flow through the grids. It treated the input of flow into the grid as positive and the flow output of the grid as negative. With this convention, the total inflows and outflows were computed for all the grids in the MZoI (modelled zone of interest) using the sum of all the positive and negative 'gflow' values. The fish module was configured according to the potential zone of interest through which the water seepage was anticipated. Histories of inflow, outflow, and qratio were set to generate plots for monitoring the convergence of the solution.

For achieving the steady state solution of seepage rate, the total inflow and outflow should converge to a common value, while the 'qratio' should approach to zero. The 'qratio' monitored here is equivalent to the 'sratio' used in the mechanical models. Hence, the 'qratio' limit was set to $10^{-5}$, and the model was solved to attain this value using the command 'solve qratio $10^{-5}$' to reach the equilibrium of the steady-state solution. The command 'SET mech off flow on' was used to calculate the steady-state seepage rate through the pillar.

A dedicated log file was created for each parameter being monitored, which was processed in Microsoft Excel for further analysis of data. As the data stored in the log files of different models was exhaustive and of a similar nature, a macro function in Microsoft Excel was prepared to automate the cleaning of the data and their faster analysis.

### 3.4.1 Assessment of Mechanical Stability

The mechanical stability of the PWBP is a primary concern for the hydro-mechanical stability of the pillar. The 'zone of positive volumetric strain (ZoPVS)' expressed in terms of the percentage of the total number of elements within the pillar was used to assess the mechanical

stability of PWBP. A FISH function developed for this purpose was called after the models achieved their final steady-state coupled equilibrium. The rate of water seepage w.r.t. the ZoPVS was studied for varying pillar width to understand the phenomenon of piping failure of the pillar.

### 3.4.2 Assessment of Hydraulic Performance

The condition of a barrier pillar deteriorates in the presence of water, and it needs a detailed investigation incorporating the combined influence of hydraulic and mechanical conditions. The flow of a large amount of water through the pre-existing fractures in the barrier pillar and its adjoining floor and roof strata at sufficiently high-velocity results in erosion of filling material, creating a smoother path that offers lesser resistance to the flow. The overall condition leads to accelerated flow carrying larger particles along with it. The continuation of this process eventually leads to piping failure of the pillar. The variation in mobility coefficient (MC) across the pillar was assessed using a FISH module developed for this purpose. The FISH module computed the updated mobility coefficient of each zone in the pillar. The average MC of all the zones in the vertical plane were obtained across the pillar and stored in the form of a table containing location across the pillar vs. average mobility coefficient. These values were later extracted in a log file and plotted in Microsoft Excel for further study.

A separate FISH module was formulated to compute the seepage rate for different flow regimes. It computed the total seepage rate from the pillar, roof, and floor edges separately as well as jointly.

## 3.5 Parametric Study

An extensive parametric study was performed for strength, pillar width, permeability, water head, and cover depth to assess the mechanical and flow response of the PWBP. The data collected from the field and literature were used to establish the ranges for the inputs to the experimental models. The study covered (a) flow through the pillar-only, (b) floor-only, (c) roof-only, (d) roof and pillar only, (e) pillar and floor only, and (f) pillar system i.e. roof, pillar and floor, to analyse the full spectrum of different geotechnical flow regimes. The results of all the numerical models were compiled to understand the underlying mechanical, hydraulic, and coupled phenomena of PWBP.

## 3.6 Development of Design Criteria and their Validation

Based on the understanding developed through literature review, field visits and laboratory studies, the criteria for delineation of piping failure and controlled seepage rate were developed considering the characteristic ZoPVS, seepage rate for pillar system, and the seepage rate severity classification developed for the Indian coal mines. The developed model was also verified for two different geo-mining conditions and compared with their field observation.

## 3.7 Summary

This chapter described the methodology adopted in this work for simulating the hydro-mechanical behaviour of PWBP in a given geo-mining condition. It discussed the approach for simulating the laboratory-observed stress-strain behaviour of coal pillars in India. The mechanism for introducing the effect of confinement on the mechanical behaviour of pillars was also considered through careful consideration of the relevant interface properties. An approach for simulating the strain-induced porosity and permeability of the rock and its effect

on the hydraulic performance of the pillars were also worked out. The effect of the zone of influence in the immediate roof and floor on its overall behaviour was also captured by considering the modelled zone of influence (MZoI). The pertinent mechanical and hydraulic boundary conditions were discussed along with the in-situ stress initialisation and solution schemes for simulating the mechanical and hydraulic behaviour of the pillar and their coupling. The standard approach for evaluating the modelling outcomes was also discussed in detail.